

is that extraction constants of $\text{Cu}(\text{DTC})_2$ are so high that practically all $\text{HDTC}_{(\text{org})}$ will be converted to $\text{Cu}(\text{DTC})_2$ and extracted easily and quantitatively into the organic layer. Thus the two-step extraction method described here provides a good way to determine the free-ligand concentration in the first step of the extraction. Radiometry incorporated into this technique makes the two-step extraction method more valuable. In principle, determination of extraction constants by the present method can be extended to other metal dithiocarbamates as long as their extraction constants are lower than that of copper dithiocarbamate (7-12).

Table III summarizes the $K_{\text{M}(\text{DTC})_m}^{\text{acid}}$ and $K_{\text{M}(\text{DTC})_m}$ values obtained in the present study. The former was experimentally observed, whereas the latter was calculated by eq 5. It is found that the extraction constants of the metal diethyldithiocarbamates are generally higher than those of the metal pyrrolidinecarbodithioates. All of the literature values are also listed in Table III for comparison.

LITERATURE CITED

- (1) Still, E. *Suom. Kemistiseuran Tied.* **1964**, *73*, 90-106.
- (2) Stary, J.; Kratzer, K. *Anal. Chim. Acta* **1968**, *40*, 93-100.

- (3) Ooms, P. C. A.; Brinkman, U. A. Th.; Das, H. A. *ECN [Rep.]* **1976**, No. 77-018.
- (4) Ooms, P. C. A.; Brinkman, U. A. Th.; Das, H. A. *Radiochem. Radioanal. Lett.* **1977**, *31*, 317-322.
- (5) Bajo, S.; Wyttenbach, A. *Anal. Chem.* **1979**, *51*, 376-378.
- (6) Likussar, W.; Boltz, D. F. *Anal. Chem.* **1971**, *43*, 1273-1277.
- (7) Wyttenbach, A.; Bajo, S. *Anal. Chem.* **1975**, *47*, 1813-1817.
- (8) Wyttenbach, A.; Bajo, S. *Anal. Chem.* **1975**, *47*, 2-7.
- (9) Bode, H.; Tusche, K. J. *Fresenius' Z. Anal. Chem.* **1957**, *157*, 414-427.
- (10) Wickbold, R. *Fresenius' Z. Anal. Chem.* **1956**, *152*, 259-262.
- (11) Eckert, G. *Fresenius' Z. Anal. Chem.* **1957**, *155*, 23-25.
- (12) Yeh, S. J.; Lo, J. M.; Shen, L. H. *Anal. Chem.* **1980**, *52*, 528-531.
- (13) Ringbom, A. "Complexation in Analytical Chemistry"; Interscience: New York/London, 1963.
- (14) Bode, H. *Fresenius' Z. Anal. Chem.* **1955**, *144*, 165-186.
- (15) Stary, J. "The Solvent Extraction of Metal Chelates"; Pergamon Press: Oxford, 1964.
- (16) van Erkelens, P. C. *Anal. Chim. Acta* **1962**, *26*, 32-45.
- (17) Kuehner, E. C.; Alvarez, R.; Paulsen, P. J.; Murphy T. J. *Anal. Chem.* **1972**, *44*, 2050-2056.
- (18) Aspila, K. I.; Sastri, V. S.; Chakrabarti, C. L. *Talanta* **1969**, *16*, 1099-1102.
- (19) Joris, S. J.; Aspila, K. I.; Chakrabarti, C. L. *Anal. Chem.* **1969**, *41*, 1441-1445.
- (20) Scharfe, R. R.; Sastri, V. S.; Chakrabarti, C. L. *Anal. Chem.* **1973**, *45*, 413-415.

RECEIVED for review June 26, 1979. Accepted June 23, 1980.

Glancing Incidence External Reflection Spectroelectrochemistry with a Continuum Source

Joan P. Skully and Richard L. McCreery*

Department of Chemistry, The Ohio State University, Columbus, Ohio 43210

A previous report demonstrated that light reflected from an electrode at small angles could be used to make optical absorption measurements on electrogenerated chromophores. A large sensitivity enhancement over previous methods was realized due to the relatively long effective path length. The present report discusses the extension of the technique to carbon and platinum electrodes and the use of a continuum rather than laser light source. For all combinations of source and electrode, the sensitivity of the method is about 100 times that of a comparable experiment using an optically transparent electrode, and the magnitude of the enhancement can be calculated from geometric considerations. In addition, the effect of the beam entering the side of the diffusion layer was considered, and it was found that this effect can be neglected if the experiment is designed properly.

The external reflection geometry has been used for spectroscopic monitoring of electrochemical events both at the electrode surface and in the nearby solution (1-4). Conventional, single-pass reflection geometries have inherently low sensitivity due to short effective optical pathlength, but recent reports describe the use of multiple reflections (5) or glancing incidence angle (6, 7) to improve the effective path length. When the light beam approaches the electrode at a small angle relative to the surface, the light traverses a path in the diffusion layer which is long compared to the path for an optically transparent electrode (OTE) operated in the usual normal incident configuration. An initial report on this approach

demonstrated sensitivity enhancements of factors of 100-200 over an OTE experiment under similar conditions (6). The importance of this enhancement lies in the fact that absorbances for OTE spectroelectrochemical experiments are very small due to the short effective pathlength and become even smaller as the time of the experiment decreases (8). While OTE approaches have been very valuable for a variety of applications, their use for short-lived electrogenerated chromophores has been limited to special cases where strong absorbers are involved or where extensive time averaging is permitted (9). When weak chromophores or irreversible chemical reactions are involved, the OTE approach may not yield results with sufficient signal to noise ratio.

Since the absorbance for an electrogenerated chromophore is time dependent, it is convenient to compare sensitivities of spectroelectrochemical techniques to that for a normal incident beam passing through an OTE. For this geometry, the absorbance for a reduced species generated from a non-absorbing oxidized species is given by eq 1 (1, 8). As shown

$$A(t) = (2/\pi^{1/2})\epsilon_{\text{Red}}C_{\text{Ox}}^{\text{bulk}}(D_{\text{Ox}}t)^{1/2} \quad (1)$$

previously (6), the absorbance measured with a reflected beam is higher by a factor of $2/(\sin \alpha)$, where α is the angle of the beam relative to the electrode. This factor will be referred to as the enhancement of absorbance relative to an OTE, and the complete equation for the reflection approach is given by eq 2. The initial work using the glancing incidence geometry

$$A(t) = \frac{2}{\sin \alpha} \left(\frac{2}{\pi^{1/2}} \right) \epsilon_{\text{Red}}C_{\text{Ox}}^{\text{bulk}}(D_{\text{Ox}}t)^{1/2} \quad (2)$$

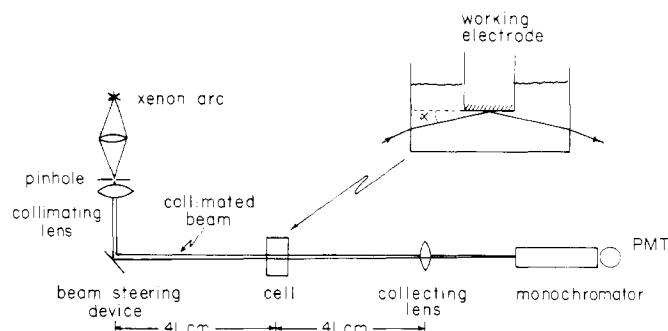


Figure 1. Apparatus for continuum source experiments. The reference and auxiliary electrodes were placed out of the beam, with no special concern for resistance effects. Inset shows a side view of the cell, with the electrode oriented horizontally and the beam approaching from below.

showed that experiment agreed with theory up to enhancements ($2/(\sin \alpha)$) of 100, although experimental enhancements up to 219 were observed (6). It should be noted that the absorbance values obtained with this technique are in the region of several tenths of units, rather than the 10^{-3} unit values obtained from comparable OTE experiments. These results were obtained with a He/Ne laser reflected off a vapor-deposited gold on glass electrode. Subsequent work in a different laboratory using a platinum electrode demonstrated agreement with theory up to an enhancement of 22, with values as high as 100 being observed (7). In addition, it was shown that the technique was applicable to the millisecond and submillisecond time frame.

While previous work indicates the promise of the glancing incidence approach, the laser source and vapor-deposited electrode impose limitations on the applicability of the method. In addition, the theory developed previously assumes that the beam traverses a path through the entire diffusion layer. At small incident angles, however, some of the beam enters the edge of the diffusion layer, yielding a smaller absorbance enhancement. The objectives of the work presented here are the evaluation of other electrode materials, development of a continuum rather than laser source, and consideration of the error caused by the light beam entering the edge of the diffusion layer.

EXPERIMENTAL SECTION

The laser-based experiments were identical with those described earlier, except for the electrode material and orientations. The polished glassy carbon and platinum electrodes were oriented horizontally, but this was a matter of convenience and had no apparent effect on the results for the time frames used. The electrode surface was aligned with respect to the beam in the same fashion as before (6). A 1.5 cm diameter vitreous (glassy) carbon disk was obtained from Atomergic Chemicals and was polished with a mechanical polisher (Buehler Minimet) using a series of abrasives. In order of use, they were silicon carbide paper (180, 240, 320, 400, 600 grit), "Metadi" diamond (15, 6, 1 μm), alumina A (0.5 μm), and alumina B (0.03 μm), all Buehler products. The final surface was highly reflective and exhibited much better electrochemical behavior than unpolished carbon for the systems examined. A 1 cm diameter Pt button electrode was polished by hand with the same compounds. The vapor-deposited gold electrode consisted of an optical flat coated with chromium (70 Å) followed by gold (3000 Å) and had a dimension of 0.8 cm along the optical axis. A Pt-wire auxiliary electrode and saturated calomel reference electrode were used in all cases.

The white-light apparatus is shown schematically in Figure 1. A 75-W xenon arc was focused on a 190- μm pinhole using the optics supplied with the arc housing (Schoeffel). A 5-cm focal length lens collimated light from the pinhole and then the beam was directed toward the cell with a beam steering device (Newport Research). After reflection off the electrode, the beam was focused onto the slit of a monochromator (Jobin-Yvon H-20) followed by

Table I. Absorbance vs. Time Results for Various Electrode/Source Combinations

	C laser	Pt laser	Au-Xe arc	C-Xe arc
incident angle, deg	1.58	1.36	1.58	1.58
predicted enhancmt ($2/\sin \alpha$)	72.5	84.3	72.5	72.5
predicted enhancmt (cor)	69.3	77.5	67.4	69.3
calcd $A/t^{1/2}$ (eq 2)	0.255	0.690	0.204	0.204
calcd $A/t^{1/2}$ (cor)	0.244	0.634	0.190	0.195
obsd $A/t^{1/2}$	0.231	0.636	0.185	0.183
obsd enhancmt	65.6	77.7	65.6	65.0

a 1P28 photomultiplier. To minimize the effects of beam divergence (about 0.04° for this source), we placed the cell closer to the steering device than it was for the laser experiments (41 vs. 113 cm). The photomultiplier signal was monitored by a computer before and after a potential step and the absorbance vs. time curve was calculated from this information. The potential was controlled by using a PARC 173 potentiostat.

Several test systems were employed, covering different regions of the spectrum. *N,N,N,N*-Tetramethyl-*p*-phenylenediamine dihydrochloride (TMPD) was oxidized to its blue cation radical at +0.2 V vs. SCE in pH 7 phosphate buffer. Previous work (10) indicates that TMPD cation radical is stable for at least 15 s and has a molar absorptivity of $4200 \text{ M}^{-1} \text{ cm}^{-1}$ at the He/Ne wavelength (632.8 nm). The TMPD oxidation was used for all laser-based experiments. For experiments using white light, potassium ferrocyanide was oxidized to ferricyanide at +0.6 V vs. SCE in 1 M KNO_3 . Its diffusion coefficient (11) is $0.632 \times 10^{-5} \text{ cm}^2/\text{s}$ and its molar absorptivity (12) is $1000 \text{ M}^{-1} \text{ cm}^{-1}$ at 425 nm. The oxidation of adrenaline was used as an example of an ECC reaction involving absorbing reactive intermediates. Adrenaline (I) is oxidized to an unstable *o*-quinone ($\lambda_{\text{max}} \approx 400 \text{ nm}$, $\epsilon \approx 975$) which reacts to form adrenochrome ($\lambda_{\text{max}} = 490 \text{ nm}$, $\epsilon \approx 2900$). The half-life of the *o*-quinone at pH 5 is about 0.7 s.

RESULTS

Theoretical and experimental results for various combinations of electrodes and sources are given in Table I. Two values for the predicted enhancement are given, one equal to $2/(\sin \alpha)$, the other corrected for entry of the beam into the side of the diffusion layer as discussed below. As shown by eq 2 the quantity $A/t^{1/2}$ should be a constant for a stable chromophore and a given experiment. In all cases, A was linear with $t^{1/2}$ for the time period from 40 ms up to several seconds. The observed $A/t^{1/2}$ in Table I is the average value for the period from 50 ms to 1 s. The first row of calculated $A/t^{1/2}$ values listed in Table I was calculated directly from eq 2, assuming a simple $2/(\sin \alpha)$ enhancement, and literature values for diffusion coefficients and molar absorptivities. The second row was calculated by using the corrected value for the enhancement. The observed enhancement is the observed absorbance divided by that calculated for an OTE experiment (eq 1).

The effect of incident angle for the white-light source on a carbon electrode is shown in Table II. These results are comparable to those for the laser/gold combination described previously, with good quantitative agreement for enhancements of 100 or less.

Absorbance vs. time transients were taken every 10 nm from 380 to 560 nm for the oxidation of adrenaline at a vitreous carbon electrode at pH 5. Two such transients are shown in Figure 2A for 400 and 490 nm, with the incident angle being 1.58° (enhancement ≈ 70). These transients are single runs with no time averaging, and show good S/N even for the

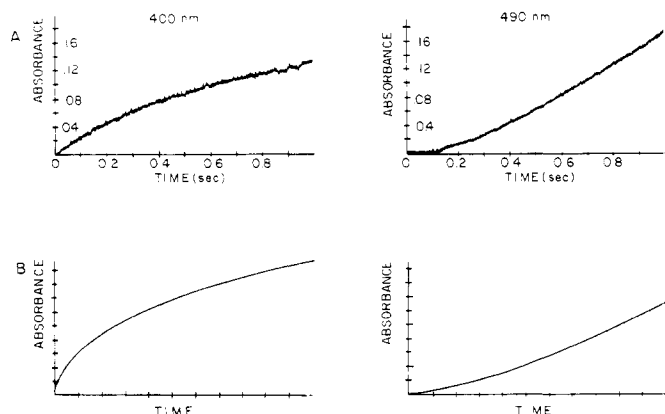


Figure 2. Absorbance vs. time transients for adrenaline oxidation at pH 5 at a carbon electrode: (A) observed transients at 400 and 490 nm; (B) simulated transients for ECC mechanism. Absorbance scale is in arbitrary units. Bulk adrenaline concentration was 1.4 mM and the incident beam angle was 1.58° .

Table II. Absorbance vs. Time Results for a Carbon Electrode and Continuum Source

incident angle, deg	2.10	1.58	1.05	0.53	0.32
predicted enhancmt ($2/(\sin \alpha)$)	54.6	72.5	109	218	364
predicted enhancmt (cor)	52.9	69.3	102	193	293
calcd $A/t^{1/2}$ (eq 2)	0.154	0.204	0.308	0.633	1.056
calcd $A/t^{1/2}$ (cor)	0.149	0.195	0.288	0.560	0.850
obsd $A/t^{1/2}$	0.155	0.183	0.283	0.352	0.401
obsd enhancmt	55.0	65.0	100	121	138

relatively weak chromophores involved. Figure 3A shows absorbance vs. wavelength spectra derived from the series of A vs. t transients. Figure 3B shows spectra of pure solutions of the *o*-quinone and adrenochrome for comparison. The *o*-quinone spectrum was obtained in 1 M HCl where adrenochrome formation is prevented, and the adrenochrome spectrum was obtained from the final product of a bulk electrolysis at pH 5.

In order to assess the importance of entry of the beam into the side of the diffusion layer, we made a theoretical exam-

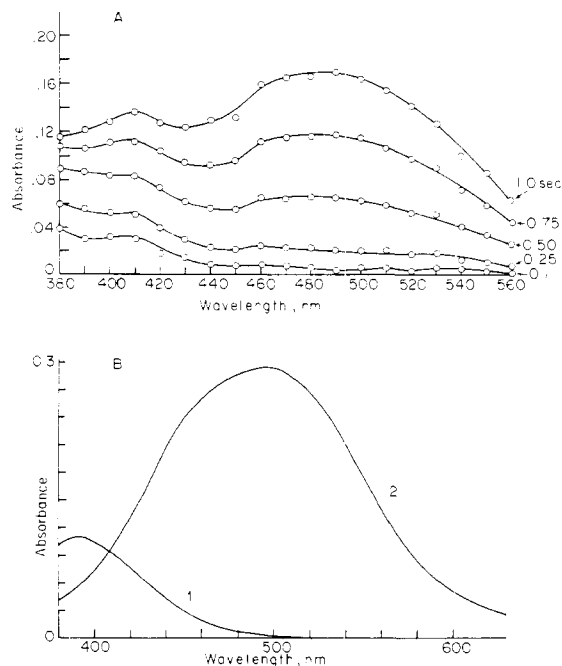


Figure 3. (A) Absorbance vs. wavelength curves at various times after initiation of adrenaline oxidation, same conditions as Figure 2. Numbers next to curves are times in seconds after the potential step. (B) Comparison spectra of adrenaline *o*-quinone at pH 0 (curve 1) and adrenochrome at pH 5 (curve 2).

ination with finite difference simulation techniques. The region near the electrode was divided into incremental regions along both axes, as shown in Figure 4. Each increment was then assumed to contain a concentration of chromophore calculated from a standard Fick's law concentration profile for stable electrogenerated material. A typical calculation divided up the diffusion layer into 1000 boxes along the axis parallel to the electrode and 1000 along the axis perpendicular to the electrode; smaller increments did not affect the results significantly. After the concentration of each box was established, the absorbance was calculated by summing the contributions to the absorbance for boxes traversed by the beam (14). Enhancements calculated by using this approach for several angles, electrode lengths, and times are listed in Table III. It should be emphasized that these results assume semiinfinite linear diffusion with no kinetic complications. The fact that the edge of the diffusion layer is not sharp, as

Table III. Effect of Time, Electrode Length, and Incident Angle on Edge Correction

time duration, s	incident angle, deg	predicted path length enhancmt ($2/(\sin \alpha)$)	corrected path length enhancement		
			electrode length = 3.5 cm	electrode length = 1.5 cm	electrode length = 0.7 cm
2	2	57.3	56.1	54.5	51.3
	1.5	76.4	74.3	71.4	65.8
	1	115	110	103	90.7
	0.7	163	154	141	115
	0.5	229	210	185	133
1	2	57.3	56.5	55.3	53.1
	1.5	76.4	74.9	72.9	68.9
	1	115	111	107	97.7
	0.7	163	157	148	129
	0.5	229	216	198	161
0.3	2	57.3	56.8	56.2	55.0
	1.5	76.4	75.6	74.5	72.3
	1	115	113	110	105
	0.7	163	160	155	145
	0.5	229	222	212	192
	0.3	382	361	334	279

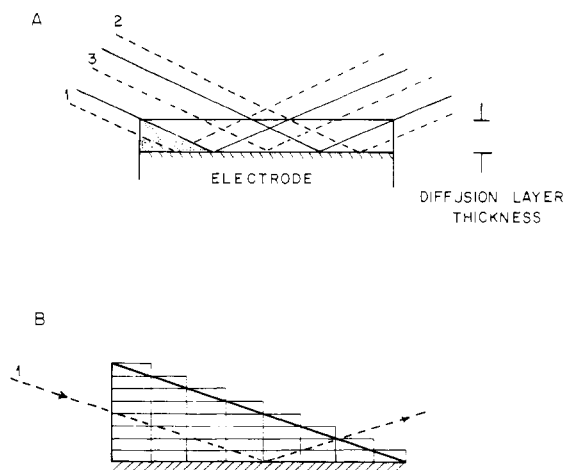


Figure 4. Incremental divisions of the diffusion layer for simulation of the effect of beam entry into the edge of the layer. Light following path 3 is not affected by edge entry and results in a $2/(\sin \alpha)$ absorbance enhancement. The absorbance due to light following path 1 or 2 was calculated by summing the contributions for the increments shown schematically in B.

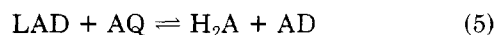
shown in Figure 4, is not important since the electrode length is long relative to the diffusion layer thickness.

DISCUSSION

The data in Tables I and II indicate that polished carbon or platinum electrodes perform as well as vapor-deposited gold for the conditions examined. Not only are the enhancements as large as reported for gold but quantitative agreement with theory allows the enhancement to be predicted from the incident angle down to 1° (enhancement = 102). The observed enhancements are closer to the theoretical values corrected for edge effects than to the simple $2/(\sin \alpha)$ value. While one would expect the polished surfaces to be rougher than the vapor-deposited gold, no effect on results was apparent, at least for time frames (longer than about 50 ms) examined here. The addition of two new electrode materials to those suitable for the glancing incidence approach expands the versatility of the method to more chemical systems and potential regions. In addition, the rugged nature and low resistance of the bulk carbon and platinum make them easier to handle and better behaved for electrochemical experiments, compared to thin film optically transparent electrodes.

Tables I and II also demonstrate that the continuum source performs as well as the laser for the glancing incident geometry. While the maximum enhancement observed with white light was somewhat lower than that of the laser (140 vs. 219), good quantitative agreement with theory prevailed up to enhancements of 100 in both cases. Since the divergence of the continuum beam was much smaller than the incident angle (0.04° vs. 1°), no apparent problems were caused by beam divergence, although one would expect such problems to appear at very small incident angles ($<1^\circ$). The nature of the source makes the continuum experiments somewhat more difficult, but the increased versatility is well worth the slightly more complex apparatus.

The adrenaline oxidation provides an excellent example of the utility of the glancing incidence technique for monitoring short-lived or weakly absorbing species. The reaction sequence has been presented by Adams et al. (13) and is summarized by eq 3-5, where H_2A represents adrenaline, AQ represents



adrenaline *o*-quinone, LAD represents leucoadrenochrome,

and AD represents adrenochrome. As indicated earlier, AQ and AD absorb in the visible wavelength region. The value of k at pH 5 is about 0.99 s^{-1} , yielding a half-life for AQ of about 0.7 s. For an OTE experiment under the same conditions as Figure 3, the absorbance for AD would be about 0.003 and for AQ about 0.002 units at 1 s. Thus, an OTE experiment would require significant time averaging, a task made more difficult by the irreversible nature of reaction 4. With the present approach, the absorbance values are 70 times the OTE values, and completely adequate S/N ratios are available from single runs.

It is not the purpose of the present work to verify the mechanism presented by eq 3-5. For comparison purposes, however, standard digital simulation techniques were used to predict absorbance vs. time curves for AQ and AD, based on the ECC mechanism. The results of these simulations are presented in Figure 2B, and it is clear that the agreement between simulation and experiment is good, indicating that the technique may be used for kinetic monitoring and mechanism diagnosis in the same fashion as an OTE, but with more versatility.

The results of Table III indicate that the correction for the beam entering the edge of the diffusion layer is most significant for small angles, short electrodes, and long times, as one would predict from geometric considerations. The need for correction was not apparent in earlier work because the electrode length was much longer (37 mm) than that used here. For a 35-mm electrode, the error at 1° and 1 s is 4% and smaller at larger angles and shorter times. Under these conditions, the error introduced by using the $2/(\sin \alpha)$ term is negligible for most purposes. However, with shorter electrodes, smaller angles, or longer times, the error can become large; e.g., at 1° , 0.7-cm electrode, and 2 s the correction equals 21%. In many experiments, it may not be possible to make the correction because uncomplicated linear diffusion may not be present. For a reactive system, the diffusion profile may be complex and an enhancement correction may not be possible without knowledge of the reaction mechanism. If significant information about the system under study is necessary to make the correction, the utility of experiments requiring correction for examining unknown systems is questionable.

One concludes that the glancing incidence reflection method is most useful when the edge correction is insignificant, and the simple $2/(\sin \alpha)$ enhancement factor applies. As a rule of thumb, the error caused by neglecting edge effects is less than 5% for a 3.5-cm electrode viewed at 1° for times up to 2 s. Shorter electrodes or smaller angles can be used at shorter times. When short-lived species are being examined, experiments will often be no longer than a few tens of milliseconds and the correction is unimportant. Thus, while the potential error caused by the beam entering the edge of the diffusion layer should be kept in mind, experimental conditions can generally be adjusted to avoid the need for corrections.

Even when the enhancement correction can be accurately applied, experimental difficulties preclude quantitative results at angles less than about 0.5° . At small angles, significant stray light, which did not reflect off the electrode, reaches the detector. This light can come directly from the source or can be diffracted from the electrode. At angles below about 0.5° stray light was extremely difficult to avoid. These effects impose a practical upper limit on quantitatively predictable enhancement of a factor of about 100, although higher values were observed.

A multiple-reflection thin-layer technique reported recently (5) will not suffer from problems associated with glancing incidence but does have some difficulties from other sources. A thin-layer cell (0.12 mm in this case) has significant IR drop

and therefore poor transient response. In addition, small changes in surface reflectance caused by potential steps or adsorption will be amplified by multiple reflections. Thus, both the multiple reflection and glancing incidence approaches lead to good sensitivity, but there will be situations where one or the other is more useful.

In conclusion, the glancing incidence specular reflection technique can be used to provide at least a factor of 100 improvement in sensitivity for spectroelectrochemical experiments using gold, platinum, and glassy carbon electrodes. The sensitivity enhancement is quantitatively predictable from experimental geometry whether or not the optical beam enters the edge of the diffusion layer, but it is usually advisable to avoid situations where an edge correction is necessary. A continuum source extends the accessible wavelength region throughout the visible and UV, greatly increasing the versatility of the method.

ACKNOWLEDGMENT

The authors thank Richard Pruiksmas for helpful discussion dealing with the edge correction.

LITERATURE CITED

- (1) Heineman, W. R. *Anal. Chem.* **1978**, *50*, 390A.
- (2) MacIntyre, J. P. E. *Adv. Electrochem. Electrochem. Eng.* **1973**, *9*
- (3) Aylmer-Kelly, A. W. B.; Bewick, A.; Cantrill, P.; Tuxford, A. M. *Faraday Diss. Chem. Soc.* **1973**, *56*, 96.
- (4) Bewick, A.; Tuxford, A. M. *Symp. Faraday Soc.* **1970**, *4*, 116.
- (5) Baumgartner, C. E.; Marks, G. T.; Aikens, D. A.; Richtol, H. H. *Anal. Chem.* **1980**, *52*, 267.
- (6) McCreery, R. L.; Pruiksmas, R.; Fagan, R. *Anal. Chem.* **1979**, *51*, 749.
- (7) Ahlberg, Elisabet; Parker, David P.; Parker, Vernon D. *Acta Chem. Scand., Ser. B* **1979**, *B33*, 762.
- (8) Kuwana, T. *Ber. Bunsenges. Phys. Chem.* **1973**, *77*, 858.
- (9) Winograd, N.; Kuwana, T. *J. Am. Chem. Soc.* **1971**, *93*, 3456.
- (10) Pruiksmas, R.; McCreery, R. L. *Anal. Chem.* **1979**, *51*, 1979.
- (11) Adams, R. N. "Electrochemistry at Solid Electrodes"; Marcel Dekker: New York, 1979; p 219.
- (12) Fasman, G. D., Ed. "Handbook of Biochemistry and Molecular Biology"; Chemical Rubber Co. Press: Cleveland, 1975; p 124.
- (13) Hawley, M. D.; Tatawadi, S. V.; Plekarski, S.; Adams, R. N. *J. Am. Chem. Soc.* **1967**, *89*, 447.
- (14) For details see: Skully, J. P. Masters Thesis, The Ohio State University, Columbus, OH, programs available upon request.

RECEIVED for review June 9, 1980. Accepted July 18, 1980.
This work was supported by grants from NSF (CHE-7828068) and NIMH (28412).

Simultaneous Determination of Tin and Lead at the Parts-per-Billion Level by Coupling Differential Pulse Anodic Stripping Voltammetry with a Matrix Exchange Method

Elio Desimoni, Francesco Palmisano,* and Luigia Sabbatini

Istituto di Chimica Analitica dell'Università di Bari, Via Amendola, 173 - 70126 Bari, Italy

The complexing properties of a citrate medium are exploited to eliminate the tin-lead interference in anodic stripping voltammetry analysis. In a citrate buffer at pH 3.9, Pb(II) can be detected at the ppb level even in the presence of a hundredfold excess of tin; the minimum observable concentration of Sn(IV) is about 0.1 ppm. On the contrary, the simultaneous detection of both metals present together at the ppb level is accomplished by coupling differential pulse anodic stripping voltammetry with a matrix exchange method.

Anodic Stripping Voltammetry (ASV) has been shown to be a well suited technique for trace determination of metal ions contaminants. However, it often suffers from interferences (1-4) which can be responsible, when not considered and eliminated, for severe reduction of the potential of the technique in multielemental analyses. In some cases (5), the problem can be simply solved by a careful selection of the deposition potential; but often drastic changes in the matrix composition and/or chemical separation steps become necessary.

In particular, lead and tin give rise, in acidic supporting electrolytes, to stripping peaks at almost exactly the same potential (6-9). This interference, as well as the strong tendency of Sn(IV) to hydrolyze (10) and polymerize, are serious obstacles for a simultaneous determination of the two elements. This problem, ignored for a long time, has been recently circumvented by introducing a separation step prior

to the ASV determination. For example, the separation of tin from lead has been accomplished by solvent extraction (13) or by coprecipitation (9) on ferric hydroxyde followed by distillation of tin as SnBr₄. The separation procedures, however, are tedious, time consuming and usually require several sample manipulations which can be responsible for incomplete recovery of the metal and/or for contamination of the sample. An alternative method for the simultaneous determination of tin and lead could consist of a selective complexation of one of the two metals (likely Sn) which would prevent the tin hydrolysis and favor the resolution of the stripping peaks for the two metals. The feasibility of this method has been demonstrated by Glodowski and Kublik (14) who investigated the influence of pyrogallol on the determination of traces of tin(IV) in the presence of lead by cyclic and stripping voltammetry at hanging-drop and thin-film mercury electrodes.

In the course of the present work, the complexing properties of citrate media (15) with respect to tin were exploited to eliminate the lead-tin interference and to perform the lead determination at the ppb level in the presence of tin. Furthermore, a peculiar procedure, based on a matrix exchange method (MEM), was successfully tested for the simultaneous determination of tin and lead both present at the ppb level.

EXPERIMENTAL

All the voltammograms were recorded on PAR 174 Polarographic Analyzer equipped with a Philips PM 8120 X-Y Recorder. A conventional three-electrode arrangement was utilized; a saturated calomel electrode (with a salt bridge) was used as the